Article

Minkowskian Approach to the Pseudorange Navigation Equations

Ramón Serrano Montesinos [1,*] and **Juan Antonio Morales-Lladosa [1,2]**

1 Departament d'Astronomia i Astrofísica, Universitat de València, 46100 Burjassot, Spain; antonio.morales@uv.es
2 Observatori Astronòmic, Universitat de València, 46980 Paterna, Spain
* Correspondence: rasemon@alumni.uv.es

Abstract: Our starting point is the covariant coordinate transformation equation of a relativistic positioning system in Minkowski space–time that maps the receiver's emission coordinates (proper times broadcast by the emitters) to its coordinates in some inertial reference frame. Bancroft's analytical (closed-form) solution to the basic pseudorange navigation equations with four emitters is recovered, and the subjacent elements are geometrically interpreted. The case of four static beacons is analysed as a clarifying situation.

Keywords: relativistic positioning systems; pseudorange navigation equations; Bancroft's closed-form solution

1. Introduction

In the context of global navigation satellite systems (GNSSs), a modern approach is that of relativistic positioning. The foundations of the theory of relativistic positioning systems (RPS) were laid down some time ago: for a genesis and perspectives, please refer to [1–4] and the references therein.

In any space–time, an RPS can be thought of as a set of four emitters A ($A = 1, 2, 3, 4$) of world-lines $\gamma_A(\tau^A)$ that broadcast their respective proper times τ^A by means of electromagnetic signals. In an RPS, the basic observable is the set of four proper times $\{\tau^A\}$ received at an event x by the user. These are the user's emission coordinates (refer to [5] for a detailed analysis, and also [6,7]). The four space $\mathcal{T} \equiv [\tau^1] \times [\tau^2] \times [\tau^3] \times [\tau^4] \approx \mathbb{R}^4$ is called the grid of the positioning system. For generalities on this concept and RPS constructions in two and three dimensions see [8,9]. Similar constructions apply to locate an emitter from a given set of coplanar receivers [10,11].

The set of four emission events $\{\gamma_A(\tau^A)\}$ at the emission times $\{\tau^A\}$ received at the event x is known as the configuration of the emitters for the event x. Suppose the four world-lines $\gamma_A(\tau^A)$ are known in an inertial coordinate system $\{x^\alpha\}$ ($\alpha = 0, 1, 2, 3$). In Minkowski space–time, the location problem consists of finding the transformation between the user's emission coordinates and its coordinates in that inertial coordinate system by solving the following algebraic system of four non-linear equations (called the null propagation equations):

$$(x - \gamma_A)^2 = 0, \quad A = 1, 2, 3, 4, \tag{1}$$

where x and $\gamma_A = O\gamma_A(\tau^A)$ are, respectively, the user and the emitters position four-vectors with respect to the origin O of $\{x^\alpha\}$. The solution to (1), which maps the user's emission coordinates to its inertial coordinates, is what we may call the RPS coordinate transformation or the RPS solution [12,13].

In the traditional approach to GNSSs, one of the basic observables is the pseudorange, which is the apparent range (distance) between the emitter and the user as inferred from

the travelling time of the signal. Neglecting gravitational, atmospheric and instrumental effects, this apparent distance differs from the Euclidean geometric distance at the time of signal emission due to synchronisation errors between emitter and user clocks (clock biases or offsets). With at least four pseudorange measurements, the receiver can estimate its position and clock bias by solving the corresponding navigation equations. In practice, this estimation is the result of a multilateration problem that is solved by iterative methods (least squares algorithms) [14,15]. Analytical or closed-form solutions are usually brought in as an initial (approximate) estimation [16]. This work is concerned only with analytical solutions, leaving aside the treatment of any source of errors due to measurement uncertainties, for which further estimation and statistical analysis are necessary (see [11,17] for an analysis in the context of source localization).

The main purpose of this paper is to bring the (non-relativistic) theoretical foundations of current GNSSs closer to the RPS approach by recovering from the RPS coordinate transformation equation [12,13] one of the classical solutions to the problem that is still in use today: Bancroft's closed-form solution (with four emitters) [18]. Abel and Chaffee [19,20] used Lorentzian geometry in their interpretation of the Bancroft algorithm, providing conditions for the existence and unicity of solutions. Bancroft's solution has been recently considered in [21,22]. However, Bancroft's characteristic elements in terms of the RPS geometric ones have not been sufficiently interpreted up to now.

We begin by explaining the notation (Section 2). We then briefly review the RPS solution (Section 3) and express Bancroft's solution using a relativistic notation (Section 4). Next, by choosing a specific value for the subsidiary vector ξ, we recover Bancroft's solution from the RPS solution (Section 5), and we provide proofs of the results in Section 6. Section 7 contains a positioning example to illustrate the correspondence between both solutions for four static emitters, and Section 8 contains constructions of the characteristic regions for this static situation. Section 9 extends these constructions by considering some of the satellites as receivers. Finally, we set out our conclusions in Section 10.

Some preliminary results of this work have been communicated at the congress Mathematical Modelling in Engineering and Human Behaviour 2023 [23].

2. Notation

The main sign conventions and notation adopted in this paper are:

(i) g is the Minkowski space–time metric with signature $(-, +, +, +)$. We use units for which the speed of light in vacuum is $c = 1$.

(ii) η is the metric volume element of g, defined by $\eta_{\alpha\beta\gamma\delta} = -\sqrt{-\det g}\,\epsilon_{\alpha\beta\gamma\delta}$, where $\epsilon_{\alpha\beta\gamma\delta}$ stands for the Levi–Civita permutation symbol: $\epsilon_{0123} = 1$. The Hodge dual operator associated with η is denoted by an asterisk $*$. For instance, in index notation (where summing over repeated indices is understood), if x, y, z are space–time vectors, one has

$$[*(x \wedge y \wedge z)]_\alpha = \eta_{\alpha\beta\gamma\delta} x^\beta y^\gamma z^\delta, \tag{2}$$

where $\wedge$ stands for the *wedge or exterior product* (defined by the antisymmetrized tensor product of antisymmetric tensors).

(iii) $i()$ denotes the interior or contracted product: that is, if x is a vector and T a covariant 2-tensor, one has $[i(x)T]_\nu = x^\mu T_{\mu\nu}$ (contracting the first left tensor index). If k is another space–time vector, then we have the following properties:

$$i(k) * (x \wedge y) = - *(k \wedge x \wedge y), \tag{3}$$
$$i(k) * (x \wedge y \wedge z) = *(k \wedge x \wedge y \wedge z). \tag{4}$$

(iv) In terms of matrices, a contravariant space–time vector is represented by a column, and a covariant vector is represented by a row. In index notation, the interior or contracted (or scalar) product of a column vector (x^α) and a row vector (y_β) is the contraction $i(x)y = x \cdot y = x^\alpha y_\alpha$. A column vector (x^α) is converted into a row vector (x_α) with the

metric: $x_\alpha = g_{\alpha\beta}x^\beta$. A matrix M acts on a column vector x yielding another column vector Mx and on a row vector y yielding another row vector yM.

3. The RPS Solution in Minkowski Space–Time

In this section, we present a brief compendium of relativistic positioning in flat space–time. For more explanations and details, please refer to [12,13].

As detailed in [12], the set of Equation (1) can be conveniently solved by referring to both the user's position x and three of the emitters, say $\{\gamma_1, \gamma_2, \gamma_3\}$, to the fourth one, γ_4:

$$y = x - \gamma_4, \tag{5}$$
$$e_a = \gamma_a - \gamma_4, \qquad a = 1, 2, 3, \tag{6}$$

and separating (1) into a quadratic equation

$$y^2 = 0, \tag{7}$$

and a system of three linear equations

$$e_a \cdot y = \Omega_a, \qquad a = 1, 2, 3, \tag{8}$$

where $\Omega_a = \frac{1}{2}(e_a)^2$ are the world-function scalars associated with the three pairs of events (γ_a, γ_4) at emission times.

Here, we consider only regular emitter configurations: that is, when the four emission events $\{\gamma_A(\tau^A)\}$ determine a three-plane Γ. According to [12], a regular emitter configuration is an emission/reception configuration iff all the relative emitter positions are space-like: that is,

$$(e_a)^2 > 0, \quad (e_a - e_b)^2 > 0. \tag{9}$$

These conditions express that the vectors defined by

$$m_A = x - \gamma_A$$

are null (1) and are all future (past) oriented: $m_A \cdot m_B < 0$, $A \neq B$. The bounds imposed by conditions (9) are called the shadows that the emitters produce to each other. The null vectors m_A and m_B become collinear ($m_A \cdot m_B = 0$) at the mutual shadows produced by γ_A and γ_B, respectively. The precise definition of the shadow that a world-line produces to another world-line was given in [24] (see also [25]).

Furthermore, $\{\gamma_A(\tau^A)\}$ is an emission (reception) configuration iff, in addition to (9), the null vector y is future (past) oriented. These conditions allow interpretation of the solutions of the null propagations Equation (1) as emission solutions.

The general solution to the underdetermined system (8) is of the form:

$$y = y_* + \lambda\chi, \tag{10}$$

where y_* is a particular solution to the system, λ is a real parameter, and

$$\chi = *(e_1 \wedge e_2 \wedge e_3) = *((\gamma_1 - \gamma_4) \wedge (\gamma_2 - \gamma_4) \wedge (\gamma_3 - \gamma_4)) \tag{11}$$

is the configuration vector of the RPS, which is orthogonal to the configuration three-plane Γ. A regular emitter configuration (at x) is said to be space-like, light-like or time-like if $\chi^2 < 0$, $\chi^2 = 0$ or $\chi^2 > 0$, respectively, at x. The regions defined by these conditions are respectively denoted as $\mathcal{C}_s$, $\mathcal{C}_l$ and $\mathcal{C}_t$. In Sections 8.1 and 8.2, we analyse these regions for the case of four static emitters.

The particular solution y_* is found by bringing in a subsidiary vector ξ such that $\xi \cdot \chi \neq 0$ (that is, transversal to the emitter configuration) and is otherwise arbitrary:

$$y_* = \frac{1}{\xi \cdot \chi} i(\xi) H, \tag{12}$$

where H is the configuration bivector

$$H = \Omega_1 E^1 + \Omega_2 E^2 + \Omega_3 E^3, \tag{13}$$

with

$$E^1 = *(e_2 \wedge e_3), \quad E^2 = *(e_3 \wedge e_1), \quad E^3 = *(e_1 \wedge e_2). \tag{14}$$

Then y_* is orthogonal to ξ, $i(\xi)y_* = 0$. Quantities Ω_a, H and χ are intrinsically related to the configuration of the emitters at x and are independent of the origin of the inertial chart $\{x^\alpha\}$.

The general solution x to the null propagation Equation (1) is obtained by introducing (10) in the main quadratic Equation (7):

$$\chi^2 \lambda^2 + 2(y_* \cdot \chi)\lambda + y_*^2 = 0, \tag{15}$$

and solving for λ. This procedure gives:

$$x = \gamma_4 + y_* + \lambda \chi, \tag{16}$$

with

$$\lambda = -\frac{y_*^2}{(y_* \cdot \chi) + \hat{\epsilon}\sqrt{\Delta}}, \tag{17}$$

where

$$\Delta = (y_* \cdot \chi)^2 - y_*^2 \chi^2, \tag{18}$$

and $\hat{\epsilon}$ is the orientation of the positioning system at the event x. The orientation $\hat{\epsilon}$ is defined as the sign of the Jacobian determinant of the coordinate transformation $\tau^A(x^\alpha)$ from inertial to emission coordinates: that is,

$$\hat{\epsilon} = sgn[*(d\tau^1 \wedge d\tau^2 \wedge d\tau^3 \wedge d\tau^4)], \tag{19}$$

with $d\tau^A = \frac{\partial \tau^A}{\partial x^\alpha} dx^\alpha$. In [12], the orientation is expressed as $\hat{\epsilon} = sgn(\chi \cdot y)$ and is determined by the configuration of the emitters as seen by the user, which is analysed in [13] in connection with the bifurcation problem as follows.

Depending on the causal character of the configuration vector χ and assuming the coordinate condition $\chi \cdot y \neq 0$, we distinguish three situations (see Figures 3–5 in [13]):

(i)   If χ is time-like, there is only one emission solution P, the other (P') is a reception solution (the events P and P' are on opposite sides of the configuration hyperplane Γ). In this case, the sign of $\hat{\epsilon}$ can be determined from the sole standard emission data $\{\gamma_A(\tau^A), \{\tau^A\}\}$.

(ii) If χ is light-like, there is only one valid emission solution (the other solution is degenerate). The sign of $\hat{\epsilon}$ can be determined from $\{\gamma_A(\tau^A), \{\tau^A\}\}$.

(iii) If χ is space-like, there are two valid emission solutions: in order to determine the sign of $\hat{\epsilon}$, additional observational information is necessary (relative positions of emitters on the user's celestial sphere).

In practical GPS applications, there is generally no bifurcation problem because the valid solution is always the one that is closest to the Earth's radius. Nevertheless, bifurcation is inherent to any time-like emitter configuration and therefore acquires importance in positioning situations beyond the proximity of the Earth.

On the other hand, the sign of Δ determines the causal character of the two-plane generated by $\{y_*, \chi\}$. It is negative when the plane is space-like, zero when the plane is

light-like, and positive when the plane is time-like. From (5) and (16), this plane is the same as that generated by $\{y, \chi\}$. Since y is light-like, this two-plane is non-space-like, and therefore, $\Delta \geq 0$. Moreover, $sgn(\Delta) = sgn[(\chi \cdot y)^2]$. Consequently, the events for which $\Delta = 0$ are those where the Jacobian determinant of $\tau^A(x^\alpha)$ vanishes ($\hat{\epsilon} = 0$); these events form the border that separates two (the front and back) coordinate domains, where $\hat{\epsilon}$ takes opposite values [13].

4. Bancroft's Solution

As mentioned earlier, we aim to bring the traditional GNSS approach closer to the RPS formalism. In this section, we express Bancroft's solution [18] using the RPS notation. In fact, Bancroft's solution, despite being based on non-relativistic concepts, incorporates four-vectors and a Minkowski-like scalar product. Nevertheless, it calls for a reinterpretation of those concepts on relativistic terms.

Bancroft first defines the user's spatial coordinates, $\vec{x}$, and those of the n satellites, $\vec{s}_i$ (for our purposes, $1 \leq i \leq n = 4$). Then he introduces the pseudorange measurements t_i made by the user with respect to each of the satellites:

$$t_i = d(\vec{x}, \vec{s}_i) + b, \tag{20}$$

where $d(\vec{x}, \vec{s}_i) = \sqrt{(x - s_i^x)^2 + (y - s_i^y)^2 + (z - s_i^z)^2}$ is the Euclidean distance between the ith satellite and the user, and b is what he calls the user clock's offset.

Reinterpreting (20) as a past light-cone equation (with the user at its vertex), we identify t_i with the coordinate time component, with respect to some inertial coordinate system $\{x^\alpha\}$, of the world-line of the ith emitter:

$$t_i \longleftrightarrow \gamma_i^t,$$

and the clock's offset b with the inertial time coordinate of the user's position four-vector x is:

$$b \longleftrightarrow t.$$

Bancroft now defines the four-vectors a_i, which we identify as the (position vectors of the) emitters' world-lines:

$$a_i = (t_i, \vec{s}_i) \longleftrightarrow \gamma_i = (\gamma_i^t, \vec{\gamma}_i), \quad i = 1, 2, 3, 4.$$

He introduces a scalar product between four-vectors $\langle a, b \rangle$, which is equivalent to the scalar product in Minkowski space–time $a \cdot b \equiv g(a, b)$ with metric signature $(-, +, +, +)$.

Bancroft's solution vector $y_{1,2} = (-b_{1,2}, \vec{x}_{1,2})$ can be readily identified with the user's position four-vector x of the RPS.

These correspondences are summarized in Table 1. Now, we are ready to write down the navigation equations solved by Bancroft using the RPS notation. These are none other than Equation (1):

$$(x - \gamma_i)^2 = x^2 - 2\gamma_i \cdot x + \gamma_i^2 = 0, \tag{21}$$

with $i = 1, 2, 3, 4$.

Table 1. Identifying Bancroft's notation and concepts with those of the RPS solution.

Bancroft			RPS
pseudorange	t_i	γ_i^t	emitter coordinate time
data vector	a_i	γ_i	emitter world-line
clock offset	b	t	user coordinate time
solution vector	$y_{1,2}$	x	user position four-vector

This system of four equations can be rewritten with the help of the following scalar:

$$\rho = \frac{1}{2}x^2, \tag{22}$$

row vectors:

$$\mathbb{1} = \begin{pmatrix} 1 & 1 & 1 & 1 \end{pmatrix}, \quad r = \begin{pmatrix} r_1 & r_2 & r_3 & r_4 \end{pmatrix}, \tag{23}$$

where

$$r_i = \frac{1}{2}\gamma_i^2, \tag{24}$$

and the following matrix:

$$\mathcal{A} = \begin{pmatrix} \gamma_1 & \gamma_2 & \gamma_3 & \gamma_4 \end{pmatrix}, \tag{25}$$

where γ_i are considered column vectors. The system (21) reads:

$$\rho\mathbb{1} - i(x)\mathcal{A} + r = 0,$$

or equivalently, provided that $\mathcal{A}$ is invertible:

$$x = \rho\, u + v, \tag{26}$$

where

$$u = \mathbb{1}\mathcal{A}^{-1}, \quad v = r\mathcal{A}^{-1}. \tag{27}$$

Squaring (26) and substituting $x^2 = 2\rho$ gives:

$$E\rho^2 + 2F\rho + G = 0, \tag{28}$$

where

$$E = u^2, \quad F = u \cdot v - 1, \quad G = v^2. \tag{29}$$

Equation (26) is Bancroft's solution to the location problem, where u and v are known from the emitters' trajectories γ_i, and ρ is obtained by solving Equation (28). Here, we can distinguish the case for which $E = 0$ (which, as we will see, corresponds to a light-like configuration of the emitters):

$$E = 0 \Rightarrow \rho = -\frac{G}{2F}, \tag{30}$$

and the cases for which $E \neq 0$ (which correspond to time-like and space-like emitter configurations):

$$E \neq 0 \Rightarrow \rho = \frac{-F \pm \sqrt{F^2 - EG}}{E}. \tag{31}$$

Bancroft does not make this distinction and implicitly assumes $E \neq 0$, his solution being Equation (26) with ρ given by (31). The following expression can be used for any value of E:

$$\rho = -\frac{G}{F \pm \sqrt{F^2 - EG}}. \tag{32}$$

5. Recovering Bancroft's Solution from the RPS Solution

In this section, the quantities E, F and G, used to express Bancroft's solution, are related to the geometric elements of the RPS statement of the location problem. The subjacent correspondence is achieved using exterior calculus in Lorentzian geometry (Minkowski space–time). For clarity, the steps of this calculation are grouped into propositions, proof of which are given in Section 6.

Proposition 1. *Let* $\mathcal{A} = (\gamma_1 \ \gamma_2 \ \gamma_3 \ \gamma_4)$ *be a matrix for which the columns are the emitters' world-lines* γ_i. *The inverse of* $\mathcal{A}$ *is given by:*

$$\mathcal{A}^{-1} = [det(\mathcal{A})]^{-1} \begin{pmatrix} \Gamma^1 \\ \Gamma^2 \\ \Gamma^3 \\ \Gamma^4 \end{pmatrix}, \tag{33}$$

the matrix entries now being row vectors

$$\Gamma^1 = - * (\gamma_2 \wedge \gamma_3 \wedge \gamma_4), \quad \Gamma^2 = *(\gamma_1 \wedge \gamma_3 \wedge \gamma_4), \tag{34}$$
$$\Gamma^3 = - * (\gamma_1 \wedge \gamma_2 \wedge \gamma_4), \quad \Gamma^4 = *(\gamma_1 \wedge \gamma_2 \wedge \gamma_3),$$

and where

$$det(\mathcal{A}) = - * (\gamma_1 \wedge \gamma_2 \wedge \gamma_3 \wedge \gamma_4) \tag{35}$$

is the determinant of $\mathcal{A}$.

On the other hand, for χ and H, we have:

Proposition 2. *The configuration vector* χ *and the bivector H of an RPS can be written as:*

$$\chi = \sum_{i=1}^{4} \Gamma^i, \tag{36}$$

and

$$H = \Omega_1 * (\gamma_2 \wedge \gamma_3) + \Omega_2 * (\gamma_3 \wedge \gamma_1) + \Omega_3 * (\gamma_1 \wedge \gamma_2) \tag{37}$$
$$+ (\Omega_3 - \Omega_1) * (\gamma_2 \wedge \gamma_4) + (\Omega_2 - \Omega_3) * (\gamma_1 \wedge \gamma_4) + (\Omega_1 - \Omega_2) * (\gamma_3 \wedge \gamma_4),$$

respectively.

Notice that $\{\Theta^i\}$, with

$$\Theta^i = [det(\mathcal{A})]^{-1} \Gamma^i, \tag{38}$$

is the dual basis of $\{\gamma_i\}$: that is, $\Theta^i(\gamma_j) = \delta^i_j$. Now we can write u and v according to (27):

$$u = [det(\mathcal{A})]^{-1} \sum_{i=1}^{4} \Gamma^i = \sum_{i=1}^{4} \Theta^i, \tag{39}$$

$$v = [det(\mathcal{A})]^{-1} \sum_{i=1}^{4} r_i \Gamma^i = \sum_{i=1}^{4} r_i \Theta^i, \tag{40}$$

and the configuration vector χ can now be written as

$$\chi = det(\mathcal{A}) \, u. \tag{41}$$

With E, F and G defined as in (29), we can state the next proposition.

Proposition 3. *Setting* $\xi = \gamma_4$, *(i) the particular solution* y_* *and the discriminant* Δ *can be written as*

$$y_* = v + r_4 \, u - \gamma_4, \tag{42}$$
$$\Delta = [det(\mathcal{A})]^2 [F^2 - E \, G], \tag{43}$$

and (ii) the RPS solution is expressed as

$$x = v + \rho \, u, \tag{44}$$

where u and v are given by (39) and (40), and

$$\rho = - \frac{G}{F + \hat{\epsilon}\mu\sqrt{F^2 - EG}}, \tag{45}$$

which is Equation (32): that is, Bancroft's solution extended to any emitter configurations, with $\mu = sgn(det(\mathcal{A}))$ and $\hat{\epsilon}$ being the orientation of the RPS at x.

On the other hand, from (41) and (42), we can write Bancroft's scalars *E*, *F* and *G*, given by (29), explicitly in terms of the RPS variables.

$$E = [det(\mathcal{A})]^{-2} \chi^2, \tag{46}$$

$$F = [det(\mathcal{A})]^{-1} \left(y_* \cdot \chi - \frac{r_4}{det(\mathcal{A})} \chi^2 \right),$$

$$G = \left(y_* - \frac{r_4}{det(\mathcal{A})} \chi + \gamma_4 \right)^2 = \left(y_* - \frac{r_4}{det(\mathcal{A})} \chi \right)^2. \tag{47}$$

In Equation (47), we have used $\gamma_4 \cdot y_* \propto H(\gamma_4, \gamma_4) = 0$, $i(\gamma_4)u = 1$, and $\gamma_4^2 = 2r_4$.

Equation (46) says that the sign of *E* provides the causal character of the emitter configuration for *x*. Therefore, $E = 0 \Leftrightarrow \chi^2 = 0$ corresponds to light-like emitter configurations, which are not covered by Bancroft's solution. In contrast, Equations (16)–(18) and their transcription using Bancroft's notation (Equations (44) and (45)) are valid for any emitter configuration.

6. Proof of the Propositions

Proof of Proposition 1. Since $\mathcal{A}^{-1}$ is defined in terms of row vectors and $\mathcal{A}$ is defined in terms of column vectors, the matrix product $\mathcal{A}^{-1}\mathcal{A}$ is straightforward. In index notation, the only non-vanishing entries of $[\mathcal{A}^{-1}\mathcal{A}]^{\alpha}{}_{\beta}$ are:

$$[\mathcal{A}^{-1}\mathcal{A}]^0{}_0 = [\mathcal{A}^{-1}\mathcal{A}]^1{}_1 = [\mathcal{A}^{-1}\mathcal{A}]^2{}_2 = [\mathcal{A}^{-1}\mathcal{A}]^3{}_3$$
$$= -\frac{1}{det(\mathcal{A})} i(\gamma_1) * (\gamma_2 \wedge \gamma_3 \wedge \gamma_4) = -\frac{1}{det(\mathcal{A})} * (\gamma_1 \wedge \gamma_2 \wedge \gamma_3 \wedge \gamma_4) = 1, \tag{48}$$

where in the last two steps, we have taken into account (4) and (35). □

Proof of Proposition 2. To obtain Equation (36), we write out (11) explicitly:

$$\chi = - * (\gamma_2 \wedge \gamma_3 \wedge \gamma_4) + *(\gamma_1 \wedge \gamma_3 \wedge \gamma_4) - *(\gamma_1 \wedge \gamma_2 \wedge \gamma_4) + *(\gamma_1 \wedge \gamma_2 \wedge \gamma_3) = \sum_{i=1}^{4} \Gamma^i.$$

And to obtain (37), we write (13) explicitly, taking into account (14). The quantities χ and *H* only depend on the relative positions between pairs of emitters at the emission times. □

Proof of Proposition 3. To derive Equation (42), we start by writing out the right-hand side of y_* using (12). Setting $\xi = \gamma_4$ and calculating the contraction $\xi \cdot \chi$ using (41), we obtain:

$$\gamma_4 \cdot \chi = det(\mathcal{A})i(\gamma_4)u = det(\mathcal{A})i(\gamma_4) \sum_{i=1}^{4} \Theta^i = det(\mathcal{A}),$$

since $i(\gamma_4)\Theta^i = \delta_4^i$. From (3) and (37), we get:

$$i(\gamma_4)H = -\Omega_1 * (\gamma_2 \wedge \gamma_3 \wedge \gamma_4) + \Omega_2 * (\gamma_1 \wedge \gamma_3 \wedge \gamma_4) - \Omega_3 * (\gamma_1 \wedge \gamma_2 \wedge \gamma_4) = \sum_{a=1}^{3} \Omega_a \Gamma^a.$$

Then, the particular solution y_* is written as

$$y_* = \frac{1}{\gamma_4 \cdot \chi} i(\gamma_4) H = [det(\mathcal{A})]^{-1} \sum_{a=1}^{3} \Omega_a \Gamma^a = \sum_{a=1}^{3} \Omega_a \Theta^a, \tag{49}$$

where, using (6) and (24), the world-function scalars $\Omega_a = \frac{1}{2}(e_a)^2$ can be expressed as:

$$\Omega_a = r_a + r_4 - \gamma_a \cdot \gamma_4 \quad (a = 1, 2, 3). \tag{50}$$

Now, by substituting (50) in (49) and using (39) and (40):

$$y_* = \sum_{a=1}^{3} \Omega_a \Theta^a = \sum_{a=1}^{3}(r_a + r_4 - \gamma_a \cdot \gamma_4)\Theta^a = \sum_{a=1}^{3} r_a \Theta^a + r_4 \sum_{a=1}^{3} \Theta^a - \sum_{a=1}^{3}(\gamma_a \cdot \gamma_4)\Theta^a$$

$$= v - r_4 \Theta^4 + r_4(u - \Theta^4) - \sum_{a=1}^{3}(\gamma_a \cdot \gamma_4)\Theta^a = v + r_4 u - 2r_4 \Theta^4 - \sum_{a=1}^{3}(\gamma_a \cdot \gamma_4)\Theta^a$$

$$= v + r_4 u - g(\gamma_4),$$

where in the last step, we have taken into account that $2r_4 = \gamma_4^2$ and that

$$g(\gamma_4) = \sum_{i=1}^{4}(\gamma_i \cdot \gamma_4)\Theta^i,$$

is the one-form metrically equivalent to γ_4.

On the other hand, to obtain (43), noting that, from (39) and (40),

$$\gamma_4 \cdot u = 1, \quad \gamma_4 \cdot v = r_4,$$

and from the definitions (29) and using (41) and (42):

$$\chi^2 = [det(\mathcal{A})]^2 E, \quad y_*^2 = G + r_4^2 E + 2r_4 F, \quad y_* \cdot \chi = det(\mathcal{A})[r_4 E + F].$$

Then,

$$\Delta = (y_* \cdot \chi)^2 - y_*^2 \chi^2 = [det(\mathcal{A})]^2 [F^2 - E\, G].$$

Substituting the above expressions in (16) and taking into account that $\chi = det(\mathcal{A})u$, we obtain (44) with

$$\rho = r_4 - \frac{G + r_4^2 E + 2r_4 F}{r_4 E + F + \hat{\epsilon}\mu\sqrt{F^2 - EG}},$$

where $\mu = sgn(det(\mathcal{A}))$. To obtain (45), multiply the denominator by $r_4 E + F - \hat{\epsilon}\mu\sqrt{F^2 - EG}$ and simplify the expression. $\square$

7. Four Static Emitters: Solutions

To illustrate the correspondence between the RPS and Bancroft's solution, in this section, we use both approaches to solve the location problem for the case of four static emitters. This is a simple but clarifying example to gain insight into the RPS terminology. For any given time t measured by an inertial observer of unit velocity e_0 ($e_0^2 = -1$, $[e_0]^\alpha = (1, 0, 0, 0)$), we choose the simple spatial arrangement of an orthogonal tetrahedron as shown in Figure 1a, where the reference emitter γ_4 is at the origin of the observer's (spatial) coordinate system $\{x^1, x^2, x^3\}$.

The essential simplification that the static situation provides is the possibility to synchronise the emitters' clocks at a given common (initial) instant. The respective proper times then become synchronised forever, which allows the representation of the static case in three-dimensional diagrams. We will come back to this point in Section 8.

(a)   (b)
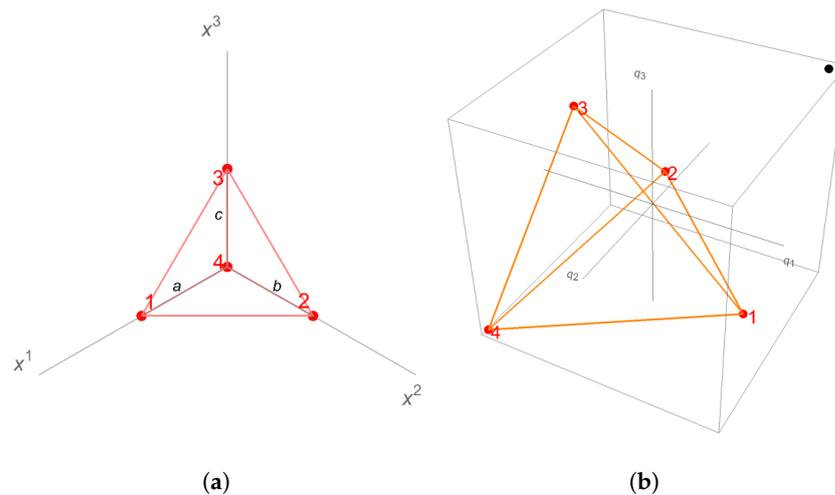
Figure 1. Representation of emitters when $a = b = c = 1$. (**a**) Spatial arrangement of four static emitters forming an orthogonal tetrahedron, with the fourth emitter at the origin. (**b**) Representation of emitters (red points) in the $\mathcal{Q}$-grid. The black (unnumbered) point has q-components $(1, 1, 1)$.

7.1. Emitters' World-Lines and Emission/Reception Conditions

As the emitters' clocks are synchronised at $x^0 = 0$ taking $\tau^1 = \tau^2 = \tau^3 = \tau^4 = 0$, the emitters' world-lines, expressed with respect to an inertial reference frame $\{x^\alpha\}$, can be easily written down in the case of static emitters:

$$\gamma_1(\tau^1) = \tau^1 e_0 + d_1, \quad \gamma_2(\tau^2) = \tau^2 e_0 + d_2, \quad \gamma_3(\tau^3) = \tau^3 e_0 + d_3, \quad \gamma_4(\tau^4) = \tau^4 e_0, \quad (51)$$

where d_a are the position vectors of the other three emitters with respect to the fourth emitter:

$$d_1 = (0, a, 0, 0), \quad d_2 = (0, 0, b, 0), \quad d_3 = (0, 0, 0, c), \quad (52)$$

where $\{a, b, c\}$ are real constants, and where we have switched to component notation, with the first component being the coordinate time x^0. We can now write the position vector of the referred emitters with respect to the reference emitter:

$$e_1 = T_1 e_0 + d_1, \quad e_2 = T_2 e_0 + d_2, \quad e_3 = T_3 e_0 + d_3, \quad (53)$$

where $T_a \equiv \tau^a - \tau^4$. Then, substituting (53) into (11), we obtain the covariant components of the configuration vector χ:

$$[\chi]_\alpha = a\,b\,c\,(-1, q_1, q_2, q_3), \quad (54)$$

where

$$q_1 = \frac{T_1}{a}, \quad q_2 = \frac{T_2}{b}, \quad q_3 = \frac{T_3}{c}.$$

The Cartesian product $\mathcal{Q} \equiv [q_1] \times [q_2] \times [q_3] \approx \mathbb{R}^3$ is included in the grid $\mathcal{T}$ of the positioning system and will be called the $\mathcal{Q}$-grid (quotient grid) according to the meaning of the triads $(q_1, q_2, q_3) \in \mathcal{Q}$ given below. Figure 1b shows the emitters' arrangement in the $\mathcal{Q}$-grid (see Equations (76) and (77)).

According to (9), the emission/reception conditions are written as

$$|q_a| < 1, \quad |aq_1 - bq_2| < \sqrt{a^2 + b^2}, \quad |aq_1 - bq_3| < \sqrt{a^2 + c^2}, \quad |bq_2 - cq_3| < \sqrt{b^2 + c^2}, \quad (55)$$

and the emission condition is written as

$$abc\lambda > 0, \quad (56)$$

with λ given by (17) in terms of y_*, χ and $\hat{\epsilon}$.

7.2. Computing the RPS Quantities

To compute the particular solution y_* (12), we begin by setting $\xi = \gamma_4 = \tau^4 e_0$:

$$\xi \cdot \chi = -\,a\,b\,c\,\tau^4. \tag{57}$$

To obtain $H = \Omega_a E^a$, we calculate the world-function scalars $\Omega_a = \frac{1}{2}(e_a)^2$ from (53):

$$\Omega_1 = \tfrac{1}{2}(a^2 - T_1^2), \quad \Omega_2 = \tfrac{1}{2}(b^2 - T_2^2), \quad \Omega_3 = \tfrac{1}{2}(c^2 - T_3^2), \tag{58}$$

and the bivectors E^a from (14), substituting (53):

$$\begin{aligned}
E^1 &= *\,(T_2 e_0 \wedge d_3) - *(T_3 e_0 \wedge d_2) + *(d_2 \wedge d_3),\\
E^2 &= *\,(T_3 e_0 \wedge d_1) - *(T_1 e_0 \wedge d_3) - *(d_1 \wedge d_3),\\
E^3 &= *\,(T_1 e_0 \wedge d_2) - *(T_2 e_0 \wedge d_1) + *(d_1 \wedge d_2).
\end{aligned} \tag{59}$$

Computing the contractions $i(\xi = \gamma_4)E^a$ using (3):

$$i(\tau^4 e_0)E^1 = (0, -\tau^4 bc, 0, 0), \ \ i(\tau^4 e_0)E^2 = (0, 0, -\tau^4 ac, 0), \ \ i(\tau^4 e_0)E^3 = (0, 0, 0, -\tau^4 ab),$$

yields the covariant components of the particular solution y_* from (12)–(14) using (57) and (58):

$$[y_*]_\alpha = \tfrac{1}{2}(0, a(1 - q_1^2), b(1 - q_2^2), c(1 - q_3^2)). \tag{60}$$

To obtain the user's inertial coordinates from (16), we need the following to calculate λ from (17):

$$\begin{aligned}
y_* \cdot \chi &= \tfrac{1}{2}abc\,[aq_1(1 - q_1^2) + bq_2(1 - q_2^2) + cq_3(1 - q_3^2)], \tag{61}\\
y_*^2 &= \tfrac{1}{4}[a^2(1 - q_1^2)^2 + b^2(1 - q_2^2)^2 + c^2(1 - q_3^2)^2], \tag{62}\\
\chi^2 &= a^2 b^2 c^2(-1 + q_1^2 + q_2^2 + q_3^2), \tag{63}
\end{aligned}$$

as follows from (54) and (60). Then, by substitution in (18),

$$\begin{aligned}
\Delta &= (y_* \cdot \chi)^2 - y_*^2 \chi^2\\
&= \tfrac{1}{4}a^2 b^2 c^2\,[2abq_1 q_2(1 - q_1^2)(1 - q_2^2) + 2acq_1 q_3(1 - q_1^2)(1 - q_3^2) + 2bcq_2 q_3(1 - q_2^2)(1 - q_3^2)\\
&\quad + a^2(1 - q_1^2)^2(1 - q_2^2 - q_3^2) + b^2(1 - q_2^2)^2(1 - q_1^2 - q_3^2) + c^2(1 - q_3^2)^2(1 - q_1^2 - q_2^2)].
\end{aligned} \tag{64}$$

Notice that Δ is an even symmetric function, $\Delta(q_1, q_2, q_3) = \Delta(-q_1, -q_2, -q_3)$, which is symmetric about the origin. With these quantities, we can express the coordinate transformation $x^\alpha(\tau^A)$ using (16)–(18).

7.3. Interpretation of the RPS Solution

In order to remark on the essential properties of the RPS solution, let us consider the inertial coordinate locations of those users whose emission coordinates satisfy the restrictions $q_1 = q_2 = q$ and $q_3 = \pm q$. Then, expressions (60)–(64) simplify, and their substitution into (16) gives:

$$x^\alpha(\tau + aq, \tau + bq, \tau \pm cq, \tau) = (\tau, 0, 0, 0) + \frac{1}{2}(1 - q^2)(0, a, b, c) + \lambda\,abc\,(1, q, q, \pm q), \tag{65}$$

with $\tau^4 \equiv \tau$: that is, $\gamma_4(\tau) = \tau e_0$, and

$$\lambda(q, q, \pm q) = -\frac{(1 - q^2)(a^2 + b^2 + c^2)}{2abc[(a + b \pm c)q + \hat\epsilon v\sqrt{q^2(a + b \pm c)^2 + (1 - 3q^2)(a^2 + b^2 + c^2)}]}, \tag{66}$$

where $\nu \equiv sgn(abc) = sgn(\chi^0)$. Then (65) will be an emission solution iff, in addition to (55) and $\Delta \geq 0$, Equation (56) holds, with λ given by (66): that is,

$$(a + b \pm c)q + \hat{\epsilon}\nu\sqrt{q^2(a+b\pm c)^2 + (1-3q^2)(a^2+b^2+c^2)} < 0. \tag{67}$$

Table 2 shows the result assuming $q_1 = q_2 = q_3 = q$ for different values of q, where for the sake of clarity, we have taken $a = b = c = 1$, and thus, $\Delta(q,q,q) = \frac{3}{4}(1-q^2)^2$.

(i)   For $q = 0$, the emitter configuration is space-like at $x^\alpha = (\tau + \frac{\sqrt{3}}{2}, \frac{1}{2}, \frac{1}{2}, \frac{1}{2})$, which is the sole emission solution (with $\hat{\epsilon} = -1$). The solution with $\hat{\epsilon} = 1$ is a reception solution.

(ii)   For $q = -\sqrt{\frac{1}{3}}$, the emitter configuration is light-like at $x^\alpha = (\tau + \frac{1}{2\sqrt{3}}, \frac{1}{6}, \frac{1}{6}, \frac{1}{6})$, which is the sole emission solution (with $\hat{\epsilon} = -1$). The solution with $\hat{\epsilon} = 1$ is degenerate.

(iii) For $q = -\sqrt{\frac{2}{3}}$, the emitter configuration is time-like at

$$x^\alpha_{\mp} = \left(\tau + \frac{\sqrt{2}\mp 1}{2\sqrt{3}}, \frac{1}{6}(\pm\sqrt{2}-1), \frac{1}{6}(\pm\sqrt{2}-1), \frac{1}{6}(\pm\sqrt{2}-1)\right),$$

both being emission solutions (with $\hat{\epsilon} = \mp 1$); $x_-(x_+)$ is in the front (back) emission coordinate domain.

Table 2. RPS solution for users with $q_1 = q_2 = q_3 \equiv q$ and $\tau^4 \equiv \tau$.

q	χ^2	Δ	x^0	$x^1 = x^2 = x^3$	Emission Solutions
0	-1	$\frac{3}{4}$	$\tau - \frac{\sqrt{3}}{2}\hat{\epsilon}$	$\frac{1}{2}$	$\hat{\epsilon} = -1$ One emission solution
$-\sqrt{\frac{1}{3}}$	0	$\frac{1}{3}$	$\tau + \frac{1}{\sqrt{3}(1-\hat{\epsilon})}$	$\frac{1}{6}$	$\hat{\epsilon} = -1$ One emission solution
$-\sqrt{\frac{2}{3}}$	1	$\frac{1}{12}$	$\tau + \frac{\sqrt{2}+\hat{\epsilon}}{2\sqrt{3}}$	$-\frac{1}{6}(1+\sqrt{2}\hat{\epsilon})$	$\hat{\epsilon} = -1, \ \hat{\epsilon} = 1$ Two emission solutions

Similarly, Table 3 shows the result assuming $q_1 = q_2 = q$ and $q_3 = -q$ for different values of q, where we have taken $a = b = c = 1$, and thus $\Delta(q,q,-q) = \frac{1}{4}(1-q^2)^2(3-8q^2)$.

Table 3. RPS solution for users with $q_1 = q_2 = q$, $q_3 = -q$ and $\tau^4 \equiv \tau$.

q	χ^2	Δ	x^0	$\dfrac{x^1 = x^2}{x^3}$	Emission Solutions
0	-1	$\frac{3}{4}$	$\tau - \frac{\sqrt{3}}{2}\hat{\epsilon}$	$\dfrac{\frac{1}{2}}{\frac{1}{2}}$	$\hat{\epsilon} = -1$ One emission solution
$-\sqrt{\frac{1}{3}}$	0	$\frac{1}{27}$	$\tau + \frac{\sqrt{3}}{2}$	$\dfrac{-\frac{1}{6}}{\frac{5}{6}}$	$\hat{\epsilon} = -1$ One emission solution
$-\sqrt{\frac{6}{17}}$	$\frac{1}{17}$	$\frac{363}{19,652}$	$\tau + \frac{11}{2}\sqrt{\frac{3}{17}}(\sqrt{2}+\hat{\epsilon})$	$\dfrac{\frac{11}{34}[1-3(2+\sqrt{2}\hat{\epsilon})]}{\frac{11}{34}[1+3(2+\sqrt{2}\hat{\epsilon})]}$	$\hat{\epsilon} = -1, \ \hat{\epsilon} = 1$ Two emission solutions

7.4. Computing Bancroft's Quantities

In order to relate the RPS and Bancroft's expression of the solution to the location problem, we begin by writing the matrix $\mathcal{A}$ given by (25), for which the columns are the emitters' world-lines (51):

$$\mathcal{A} = (\tau^1 e_0 + d_1; \tau^2 e_0 + d_2; \tau^3 e_0 + d_3; \tau^4 e_0). \tag{68}$$

In component notation, we have:

$$\mathcal{A} = \begin{pmatrix} \tau^1 & \tau^2 & \tau^3 & \tau^4 \\ a & 0 & 0 & 0 \\ 0 & b & 0 & 0 \\ 0 & 0 & c & 0 \end{pmatrix}. \tag{69}$$

To calculate $\mathcal{A}^{-1}$, we verify that:

$$\begin{aligned} det(\mathcal{A}) &= - *(\gamma_1 \wedge \gamma_2 \wedge \gamma_3 \wedge \gamma_4) \\ &= - *[(\tau^1 e_0 + d_1) \wedge (\tau^2 e_0 + d_2) \wedge (\tau^3 e_0 + d_3) \wedge \tau^4 e_0] \\ &= - \tau^4 * (d_1 \wedge d_2 \wedge d_3 \wedge e_0) = \tau^4\, a\, b\, c\, \eta_{0123} = -\tau^4\, a\, b\, c\,, \end{aligned} \tag{70}$$

and that the row vectors (1-forms) Γ^i appearing in (33) and given by (34) are expressed as:

$$\begin{aligned} \Gamma^1 &= - bc\tau^4\theta^1, \quad \Gamma^2 = -ac\tau^4\theta^2, \quad \Gamma^3 = -ab\tau^4\theta^3, \\ \Gamma^4 &= - abc\theta^0 + bc\tau^1\theta^1 + ac\tau^2\theta^2 + ab\tau^3\theta^3, \end{aligned} \tag{71}$$

where $\{\theta^0, \theta^1, \theta^2, \theta^3\}$ is the dual basis of the inertial Cartesian basis.

Now we can write $\mathcal{A}^{-1}$ as:

$$\mathcal{A}^{-1} = \begin{pmatrix} 0 & \frac{1}{a} & 0 & 0 \\ 0 & 0 & \frac{1}{b} & 0 \\ 0 & 0 & 0 & \frac{1}{c} \\ \frac{1}{\tau^4} & -\frac{\tau^1}{\tau^4 a} & -\frac{\tau^2}{\tau^4 b} & -\frac{\tau^3}{\tau^4 c} \end{pmatrix}, \tag{72}$$

and then we compute the vector u and verify (41):

$$\begin{aligned} [u]_\alpha &= [det(\mathcal{A})]^{-1} \sum_{i=1}^4 \Gamma^i = (\tfrac{1}{\tau^4}, \tfrac{1}{a}(1 - \tfrac{\tau^1}{\tau^4}), \tfrac{1}{b}(1 - \tfrac{\tau^2}{\tau^4}), \tfrac{1}{c}(1 - \tfrac{\tau^3}{\tau^4})) \\ &= \tfrac{1}{\tau^4}(1, -q_1, -q_2, -q_3) = \tfrac{1}{det(\mathcal{A})}\,[\chi]_\alpha. \end{aligned} \tag{73}$$

The vector v is obtained from (40) by substitution of (70), (71) and (24) with

$$r_1 = \tfrac{1}{2}(a^2 - (\tau^1)^2), \quad r_2 = \tfrac{1}{2}(b^2 - (\tau^2)^2), \quad r_3 = \tfrac{1}{2}(c^2 - (\tau^3)^2), \quad r_4 = -\tfrac{1}{2}(\tau^4)^2. \tag{74}$$

After simplification, the result is:

$$[v]_\alpha = \tfrac{1}{2}(-\tau^4, a - \tau^1 q_1, b - \tau^2 q_2, c - \tau^3 q_3). \tag{75}$$

We can substitute (73)–(75) and $\gamma_4 = \tau^4 e_0$ in Equation (42) and check that it is satisfied.

To compute the user's coordinates from Bancroft's solution (26) with ρ as in (31) or (32), we need the following expressions for E, F and G, which follow from (73) and (75) by the scalar product:

$$E = u^2 = \tfrac{1}{(\tau^4)^2}(-1 + q_1^2 + q_2^2 + q_3^2).$$

$$F = u \cdot v - 1 = -\tfrac{1}{2}[1 + \tfrac{q_1}{\tau^4}(a - \tau^1 q_1) + \tfrac{q_2}{\tau^4}(b - \tau^2 q_2) + \tfrac{q_3}{\tau^4}(c - \tau^3 q_3)].$$

$$G = v^2 = \tfrac{1}{4}[-(\tau^4)^2 + (a - \tau^1 q_1)^2 + (b - \tau^2 q_2)^2 + (c - \tau^3 q_3)^2].$$

Notice that Bancroft's quantities E, F and G involve the emission coordinates $\{\tau^A\}$ in addition to $\{q_1, q_2, q_3\}$. In contrast, the RPS quantities χ^2, y_*^2 and $\chi \cdot y_*$ are polynomial functions only of the $\{q_a\}$ variables. This property simplifies the representation of the RPS regions in the $\mathcal{Q}$-grid, which is carried out in the next section.

8. Four Static Emitters: Representations

In this section, we continue with the preceding example. The characteristic regions of the RPS solution are represented both in Cartesian and in emission coordinates.

8.1. Representations in Cartesian Coordinates

Figure 2 shows for a given x^0 value (inertial instant) the emission configuration regions $\mathcal{C}_s$ (space-like), $\mathcal{C}_l$ (light-like) and $\mathcal{C}_t$ (time-like), which are coloured in green, red and blue, respectively. The $\mathcal{C}_t$ region is the union of two disjoint regions, denoted by $\mathcal{C}_t$-front and $\mathcal{C}_t$-back, separated by the 3-surface $\Delta(x^0, x^1, x^2, x^3) = 0$, which is shown in black. This 3-surface, where the Jacobian determinant of $\tau^A(x^\alpha)$ vanishes, is the border between the front ($\mathcal{C}_s \cup \mathcal{C}_l \cup \mathcal{C}_t$-front) and the back ($\mathcal{C}_t$-back) coordinate domains. The union of both disjoint domains is called the emission coordinate region $\mathcal{C}$ [12,13].
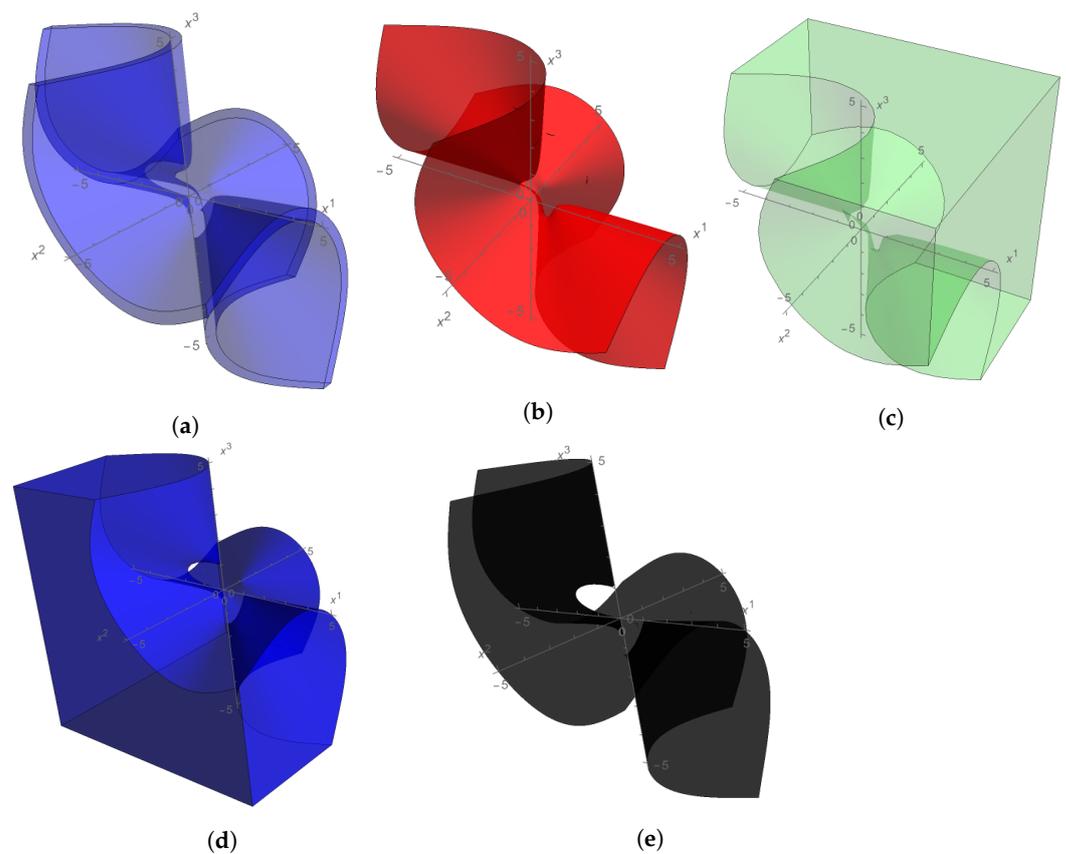

Figure 2. Representation of the emission configuration regions for an RPS with four static emitters (when $a = b = c = 1$). The emission configuration regions $\mathcal{C}_s$ (space-like), $\mathcal{C}_l$ (light-like) and $\mathcal{C}_t$ (time-like) are coloured green, red and blue, respectively. The 3-surface where Δ vanishes is shown in black. (**a**) $\mathcal{C}_t$ (front). (**b**) $\mathcal{C}_l$. (**c**) $\mathcal{C}_s$. (**d**) $\mathcal{C}_t$ (back). (**e**) $\Delta = 0$.

Figure 3 includes two-dimensional slices of the emission configuration regions shown in Figure 2. The black points represent the satellite trajectories. The intersection with $\Delta = 0$ is also represented.

(a)

(b)

(c)

(d)
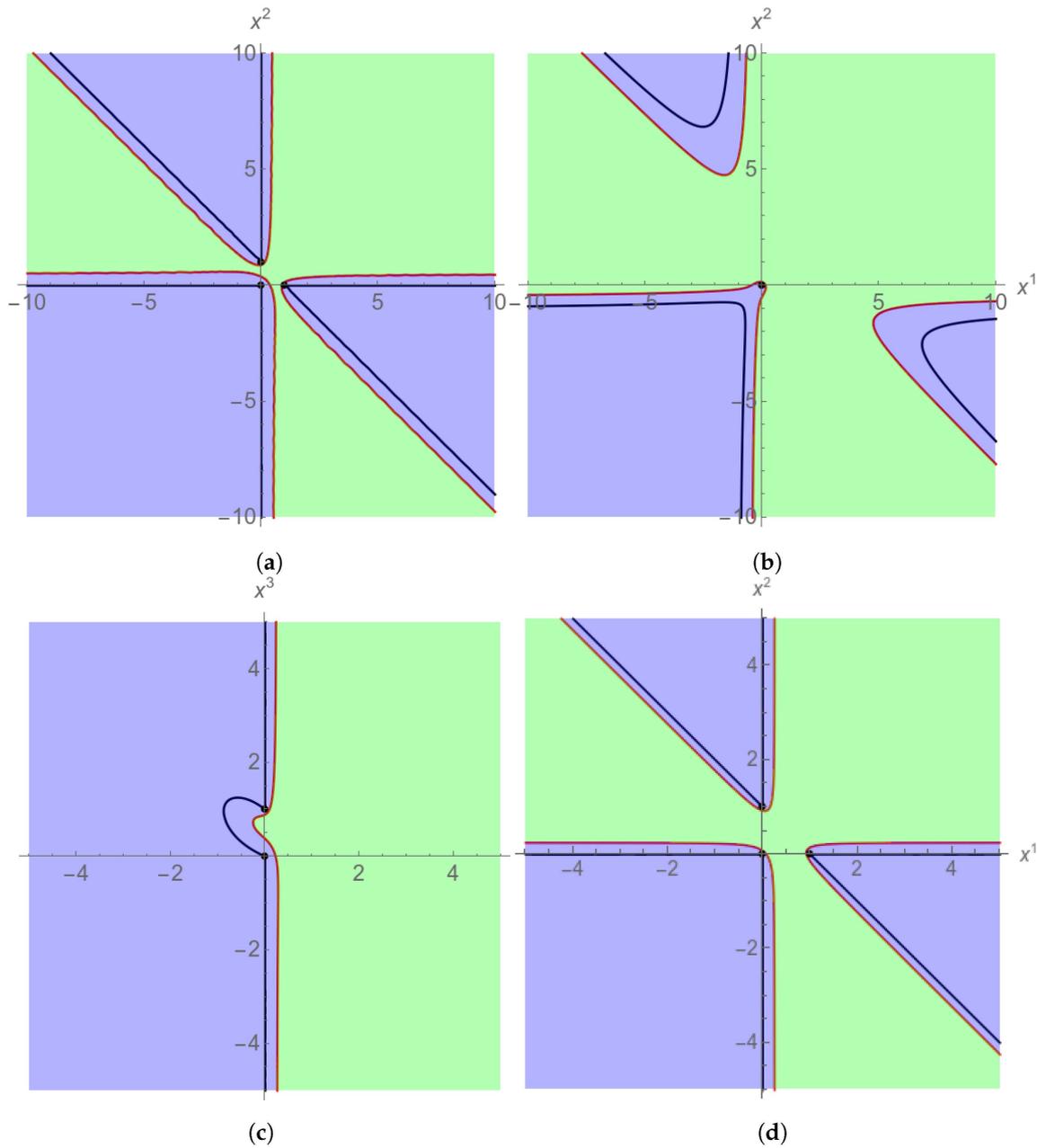
Figure 3. Slices of the emission configuration regions (shown in Figure 2) through different 2-planes. Black points represent the satellites. (**a**) Slice through the plane $x^3 = 0$. Satellites 4, 1 and 2 are represented by points $(0,0)$, $(1,0)$ and $(0,1)$, respectively. (**b**) Slice through the plane $x^3 = 1$. The point $(0,0)$ represents satellite 3. (**c**) Slice through the plane $x^1 - x^2 = 0$. Satellites 4 and 3 are represented by points $(0,0)$ and $(0,1)$, respectively. (**d**) Slice through the plane $x^1 + x^2 + x^3 = 1$. Satellites 1, 2 and 3 are represented by points $(1,0)$, $(0,1)$ and $(0,0)$, respectively.

8.2. Representations in the Q-Grid

Since the emitters' trajectories $\{\gamma_A\}$ in inertial coordinates are known from (51), we can obtain their positions S_A in the $\mathcal{Q}$-grid as well as their trajectories γ_A in the grid $\mathcal{T}$. For $a = b = c = 1$, we have

$$S_1 = (1, 1 - \sqrt{2}, 1 - \sqrt{2}), \quad S_2 = (1 - \sqrt{2}, 1, 1 - \sqrt{2}), \tag{76}$$

$$S_3 = (1 - \sqrt{2}, 1 - \sqrt{2}, 1), \quad S_4 = (-1, -1, -1), \tag{77}$$

and

$$\gamma_1 = (1+\tau, 1-\sqrt{2}+\tau, 1-\sqrt{2}+\tau, \tau), \quad \gamma_2 = (1-\sqrt{2}+\tau, 1+\tau, 1-\sqrt{2}+\tau, \tau),$$
$$\gamma_3 = (1-\sqrt{2}+\tau, 1-\sqrt{2}+\tau, 1+\tau, \tau), \quad \gamma_4 = (-1+\tau, -1+\tau, -1+\tau, \tau), \quad \text{with } \tau = \tau^4,$$

which are straight lines in the direction defined by $(1,1,1,1) \in \mathcal{T}$. In other words, the (parallel) emitter world-lines are represented as parallel lines in the grid $\mathcal{T}$ along the direction defined by the main bisectrix. Each γ_A is represented by the corresponding point S_A in the quotient grid $\mathcal{Q}$. Figure 1b is a representation of the emitters in the $\mathcal{Q}$-grid.

The boundary of the emission/reception conditions (55) defines twelve 2-planes in the $\mathcal{Q}$-grid, which are denoted by S_{AB}, $A \neq B$. S_{AB} is the representation in the $\mathcal{Q}$-grid of the shadow that satellite A produces to satellite B. Concretely, for $a = b = c = 1$, we have

$$
\begin{array}{llll}
S_{12} : q_1 - q_2 = \sqrt{2}, & S_{13} : q_1 - q_3 = \sqrt{2}, & S_{14} : q_1 = 1, \\
S_{21} : q_1 - q_2 = -\sqrt{2}, & S_{23} : q_2 - q_3 = \sqrt{2}, & S_{24} : q_2 = 1, \\
S_{31} : q_1 - q_3 = -\sqrt{2}, & S_{32} : q_2 - q_3 = -\sqrt{2}, & S_{34} : q_3 = 1, \\
S_{41} : q_1 = -1, & S_{42} : q_2 = -1, & S_{43} : q_3 = -1.
\end{array}
\tag{78}
$$

Figure 4 contains representations in the $\mathcal{Q}$-grid for $a = b = c = 1$. Figure 4a represents the convex polyhedron formed by pieces of the twelve satellite shadows (78). It has $12 = 6 + 6$ faces (six squares with side length $\sqrt{2}$ and six rhomboids with side lengths $\sqrt{2}$ and $2(\sqrt{2} - 1)$): that is, it is a dodecahedron, which we may call the shadow-dodecahedron $\mathcal{D}$. The fourteen vertices of $\mathcal{D}$ are, apart from S_4 and $-S_4$, the following points:

$$
\begin{array}{lll}
V_1 = (1, 1, 1-\sqrt{2}), & V_2 = (1, 1-\sqrt{2}, 1), & V_3 = (1-\sqrt{2}, 1, 1), \\
V_4 = (1, 1-\sqrt{2}, 1-\sqrt{2}), & V_5 = (1-\sqrt{2}, 1, 1-\sqrt{2}), & V_6 = (1-\sqrt{2}, 1-\sqrt{2}, 1)
\end{array}
$$

and their opposites. The interior of $\mathcal{D}$ contains the $\mathcal{Q}$-grid points that satisfy the emission/reception conditions (55). Figure 4b shows the surface where the Jacobian determinant of the coordinate transformation $\tau^A(x^\alpha)$ vanishes; equivalently, $\Delta(q_1, q_2, q_3) = 0$ in the $\mathcal{Q}$-grid. This surface is strictly confined inside $\mathcal{D}$. The interior of this surface satisfies $\Delta(q_1, q_2, q_3) > 0$ and corresponds to solutions of the null propagation equations. The region inside $\mathcal{D}$ satisfying $\Delta(q_1, q_2, q_3) < 0$ does not represent any physical region in the $\mathcal{Q}$-grid.


(**a**)　　　　　　　　　　　　　　　(**b**)
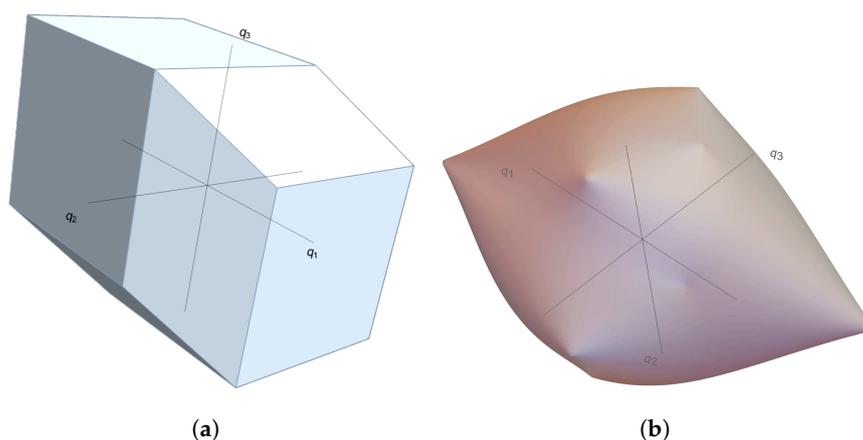
Figure 4. *Cont.*
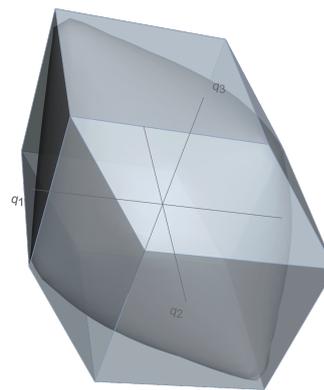
(**c**)

Figure 4. Representation of the surface $\Delta(q_1, q_2, q_3) = 0$ in the $\mathcal{Q}$-grid region where the emission/reception conditions are satisfied (with $a = b = c = 1$) and which is bounded by $\mathcal{D}$. (**a**) Shadow-dodecahedron $\mathcal{D}$. (**b**) The surface $\Delta = 0$. (**c**) The surface $\Delta = 0$ within the shadow-dodecahedron $\mathcal{D}$.

Figure 5 shows two-dimensional slices of the configuration regions in the $\mathcal{Q}$-grid when applying the emission/reception conditions (55) for $a = b = c = 1$. The colours green, red and blue are used for the space-like, light-like and time-like character of the configuration, respectively. The black lines are different slices of the 2-surface $\Delta(q_1, q_2, q_3) = 0$. For clarity, the intersections with the shadow-dodecahedron are not shown.
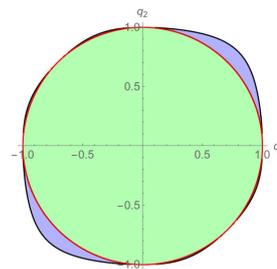

(**a**) $q_3 = 0$
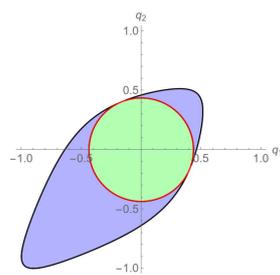

(**b**) $q_3 = -0.9$
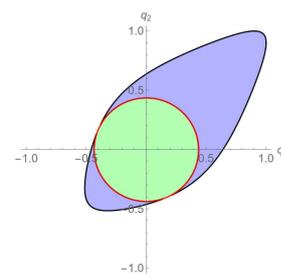
(**c**) $q_3 = 0.9$
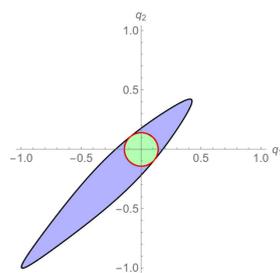
(**d**) $q_3 = -0.99$

(**e**) $q_3 = 0.99$

Figure 5. *Cont.*

(f) $q_3 = -0.999$

(g) $q_3 = 0.999$

(h) $q_3 = -1$

(i) $q_3 = 1$
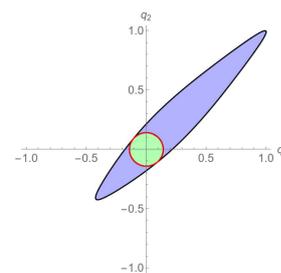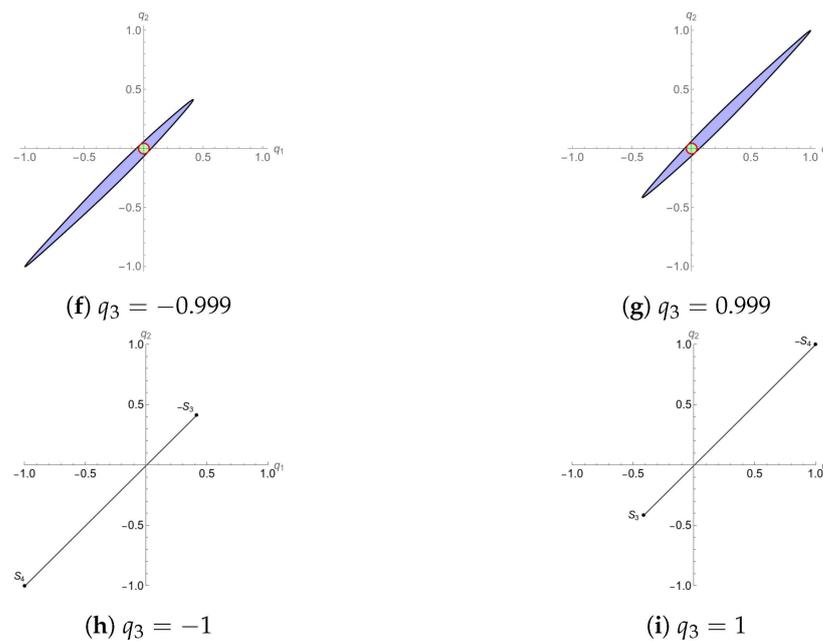
Figure 5. Representation of the emitter configuration regions in the $\mathcal{Q}$-grid for different values of q_3 when $a = b = c = 1$. The colours green, red and blue are used for the space-like, light-like and time-like character of the configuration, respectively. The black lines are different level cuts of the 2-surface $\Delta(q_1, q_2, q_3) = 0$. For $q_3 = -1$ ($q_3 = 1$), the points shown are S_4 and $-S_3$ (S_3 and $-S_4$), with S_3 and S_4 being the third and fourth satellites, respectively, given by (77).

9. Emission–Reception Conditions and Grid Regions

Figures 1b, 4 and 5 provide representations in the $\mathcal{Q}$-grid of the standard positioning data and the elements derived from these data. In this section, we use the $\mathcal{Q}$-grid representations to obtain further information about other regions where solutions to the null propagation Equation (1) exist without imposing all of the emission/reception conditions (55). We analyse a mixture of emission and reception conditions that apply to other location systems [1,2] based on null coordinates, such as reception or radar coordinates. For an analysis of the notion of a location system (physical realization of a coordinate system), see [9] and previous references quoted herein.

Figure 6 shows the surfaces in the $\mathcal{Q}$-grid defined by $\Delta(q_1, q_2, q_3) = 0$, in whose interior there is a solution to the null propagation equations. There exist fifteen disjoint regions satisfying $\Delta > 0$. The exterior of this surface ($\Delta < 0$) has no physical meaning. The interior ($\Delta > 0$) is the $\mathcal{Q}$-grid representation of the solutions to the null propagation equations and is disjointly divided into fifteen regions. Only one region contains the origin, and it is divided in two subregions where all the emission/reception conditions are satisfied (see Figure 4). Among the fourteen remaining regions, eight satisfy only three emission/reception conditions (each one is confined by three pairs of parallel planes). The other six satisfy only two emission/reception conditions (each one is confined by two pairs of parallel planes).

Table 4 shows the signs of the products $m_A \cdot m_B$ ($A \neq B$) and the related regions. The emission or reception character of a τ^A-coordinate is denoted by e or r, respectively.
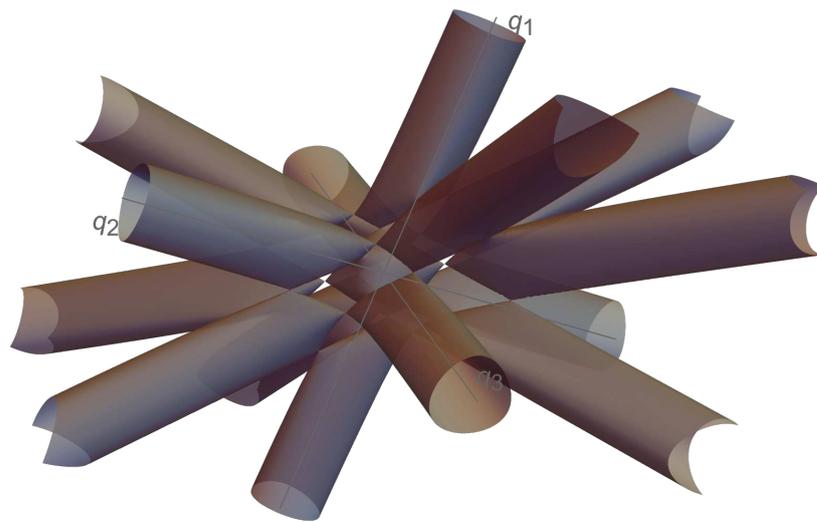
Figure 6. Representation of the surface $\Delta(q_1, q_2, q_3) = 0$ in the $\mathcal{Q}$-grid for $a = b = c = 1$. The closed piece at the centre is represented in Figure 4.

Table 4. Regions according to the sign of the products $m_A \cdot m_B$ ($A \neq B$). The emission or reception character of a τ^A-coordinate is denoted by e or r, respectively. The subregions $\{eeee\}$ and $\{rrrr\}$ form one region containing the origin (closed piece at the centre of Figure 6). The other fourteen regions correspond to the fourteen tube-like pieces emerging from the central piece in Figure 6.

$m_1 \cdot m_2$	$m_1 \cdot m_3$	$m_1 \cdot m_4$	$m_2 \cdot m_3$	$m_2 \cdot m_4$	$m_3 \cdot m_4$	Character
−	−	−	−	−	−	$\{eeee\}, \{rrrr\}$
−	−	+	−	+	+	$\{eeer\}, \{rrre\}$
−	+	−	+	−	+	$\{eere\}, \{rrer\}$
+	−	−	+	+	−	$\{eree\}, \{rerr\}$
+	+	+	−	−	−	$\{reee\}, \{errr\}$
−	+	+	+	+	−	$\{eerr\}, \{rree\}$
+	−	+	+	−	+	$\{erer\}, \{rere\}$
+	+	−	−	+	+	$\{erre\}, \{reer\}$

The results of this section may be compared with those presented in [10,11] regarding the 2D localization of a source with three receivers. In particular, there is an interesting similarity between the surface of the vanishing Jacobian (Figure 6) and the Kummer surface represented in Figure 4 of [11]. The surface shown in Figure 6 has a total of thirty-two singular points—eight of them on the central piece and twenty-four on the tube-like pieces—with each of these points connecting the different pieces that make up the surface. In addition to S_A and $-S_A$, the surface has the following singular points:

$$
\begin{array}{lll}
N_1 = (-1, 1, 1), & N_2 = (1, -1, 1), & N_3 = (1, 1, -1), \\
N_4 = (1, 1 - \sqrt{2}, 1 + \sqrt{2}), & N_5 = (1 - \sqrt{2}, 1, 1 + \sqrt{2}), & N_6 = (1 - \sqrt{2}, 1 + \sqrt{2}, 1), \\
N_7 = (1, 1 + \sqrt{2}, 1 - \sqrt{2}), & N_8 = (1 + \sqrt{2}, 1, 1 - \sqrt{2}), & N_9 = (1 + \sqrt{2}, 1 - \sqrt{2}, 1), \\
N_{10} = (1, 1 + \sqrt{2}, 1 + \sqrt{2}), & N_{11} = (1 + \sqrt{2}, 1, 1 + \sqrt{2}), & N_{12} = (1 + \sqrt{2}, 1 + \sqrt{2}, 1),
\end{array}
$$

and their opposites. Of these singular points, only S_4 and $-S_4$ are also vertices of $\mathcal{D}$.

Figure 7 shows the cuts of the surface $\Delta(q_1, q_2, q_3) = 0$ with the different planes $q_3 = constant$. Similar cuts are obtained for constant values of q_1 or q_2.
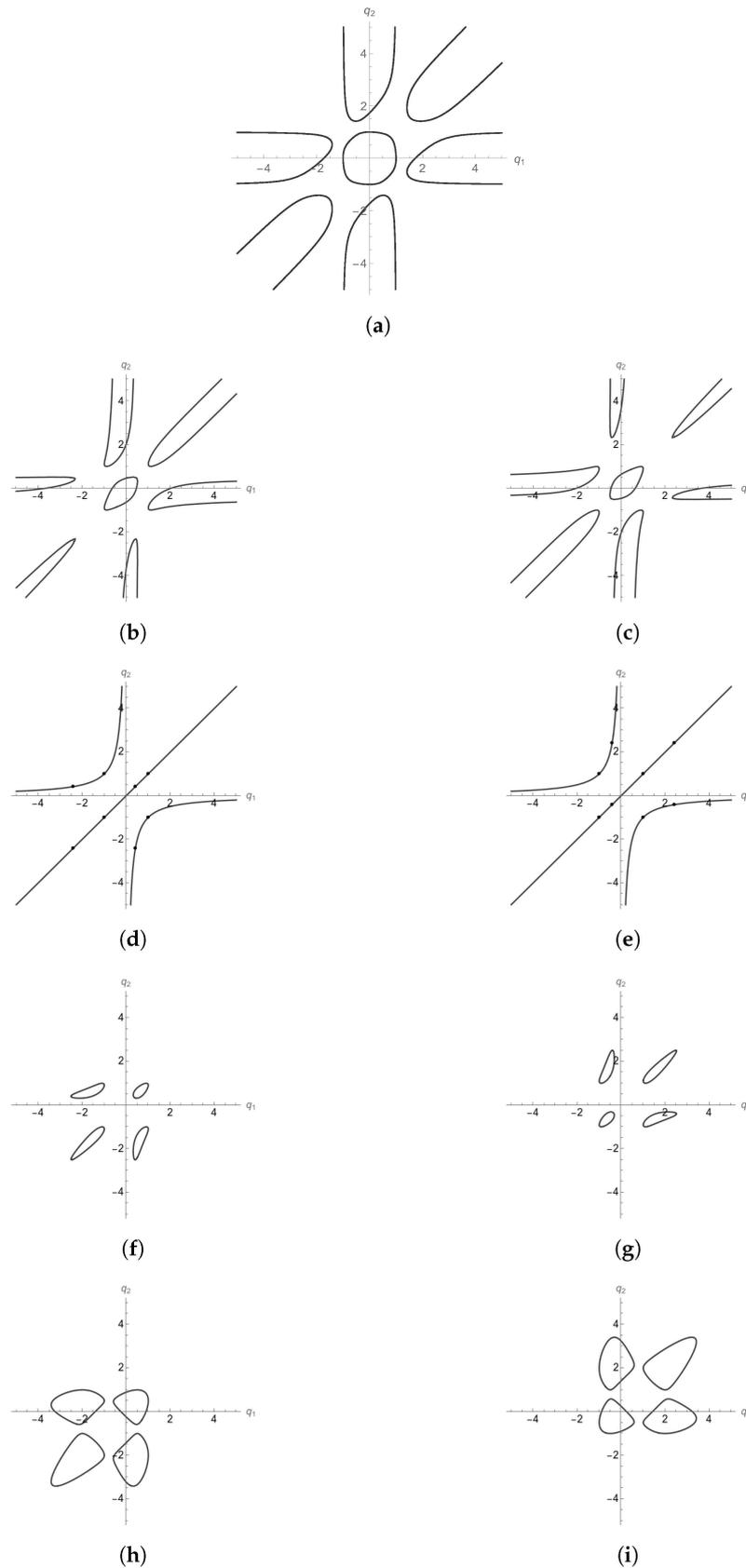
Figure 7. Representation in the $\mathcal{Q}$-grid of the level lines $\Delta(q_1, q_2, q_3 = k) = 0$ for different values of k and with $a = b = c = 1$. The points in Figures 7d and 7e are singular points. (**a**) $q_3 = 0$. (**b**) $q_3 = -0.9$. (**c**) $q_3 = 0.9$. (**d**) $q_3 = -1$. (**e**) $q_3 = 1$. (**f**) $q_3 = -1.1$. (**g**) $q_3 = 1.1$. (**h**) $q_3 = -2$. (**i**) $q_3 = 2$.

10. Conclusions

The RPS approach to GNSSs is grounded in the fundamental principles of relativity, on which, one might think, navigation systems should be based. Current GNSSs rely on a posteriori corrections for (special) relativistic effects (and for gravitational, atmospheric and instrumental effects). In this paper, we have deduced a classical solution to the navigation equations—Bancroft's solution, which is still in use today—within a relativistic framework. In fact, Bancroft's closed-form solution is suitable for this purpose since it already incorporates four-vectors and a Minkowski scalar product, although it still presumes a universal time and a deviation from it (the clock offset). We have recovered Bancroft's solution from the RPS solution using the language of relativity: contravariant (column) and covariant (row) vectors, their inner (scalar) product and their exterior algebra.

The characteristic elements of an RPS (emission and configuration regions, front and back coordinate domains, shadows produced by the satellites to each other, etc.) have been exemplified for the static situation. These regions are represented both in the physical and in the grid space of the RPS by introducing an appropriate quotienting procedure. This kind of representation has been tentatively studied for other location systems for which not all the emission/reception conditions are assumed. However, to deal with general location systems, the RPS terminology should be appropriately adapted.

All of this is with the hope of bringing the traditional GNSS approach closer to the framework of Relativity Theory: a worthwhile task, if only from a scientific perspective.

Data Availability Statement: No new data were created or analyzed in this study. Data sharing is not applicable to this article.

Conflicts of Interest: The authors declare no conflicts of interest.

References

1. Coll, B. Relativistic positioning systems: Perspectives and prospects. *Acta Futura* **2013**, *7*, 35–47. [CrossRef]
2. Coll, B. *Epistemic Relativity: An Experimental Approach to Physics*; Springer International Publishing: Berlin/Heidelberg, Germany, 2019; pp. 291–315. [CrossRef]
3. Coll, B. *Elements for a Theory of Relativistic Coordinate Systems: Formal and Physical Aspects*; World Scientific: Singapore, 2001; pp. 53–65. [CrossRef]
4. Bahder, T.B. Navigation in curved space-time. *Am. J. Phys.* **2001**, *69*, 315–321. [CrossRef]
5. Coll, B.; Pozo, J.M. Relativistic positioning systems: The emission coordinates. *Class. Quantum Gravity* **2006**, *23*, 7395. [CrossRef]
6. Rovelli, C. GPS observables in general relativity. *Phys. Rev. D* **2002**, *65*, 044017. [CrossRef]
7. Blagojević, M.; Garecki, J.; Hehl, F.W.; Obukhov, Y.N. Real null coframes in general relativity and GPS type coordinates. *Phys. Rev. D* **2002**, *65*, 044018. [CrossRef]
8. Pozo, J. Constructions in 3D (I) and (II). In Proceedings of the School on Relativistic Coordinates, Reference and Positioning Systems, Salamanca, Spain, 21–25 January 2005.
9. Coll, B.; Ferrando, J.J.; Morales, J.A. Two-dimensional approach to relativistic positioning systems. *Phys. Rev. D* **2006**, *73*, 084017. [CrossRef]
10. Compagnoni, M.; Notari, R.; Antonacci, F.; Sarti, A. A comprehensive analysis of the geometry of TDOA maps in localization problems. *Inverse Probl.* **2014**, *30*, 035004. [CrossRef]
11. Compagnoni, M.; Notari, R.; Ruggiu, A.A.; Antonacci, F.; Sarti, A. The Algebro-geometric Study of Range Maps. *J. Nonlinear Sci.* **2017**, *27*, 99–157. [CrossRef]
12. Coll, B.; Ferrando, J.J.; Morales-Lladosa, J.A. Positioning systems in Minkowski spacetime: From emission to inertial coordinates. *Class. Quantum Gravity* **2010**, *27*, 065013. [CrossRef]
13. Coll, B.; Ferrando, J.J.; Morales-Lladosa, J.A. Positioning systems in Minkowski space-time: Bifurcation problem and observational data. *Phys. Rev. D* **2012**, *86*, 084036. [CrossRef]
14. Strang, G.; Borre, K. *Linear Algebra, Geodesy, and GPS*; Wellesley-Cambridge Press: Wellesley, MA, USA, 1997.

15.   Closas, P.; Gusi-Amigo, A. Direct Position Estimation of GNSS Receivers: Analyzing main results, architectures, enhancements, and challenges. *IEEE Signal Process. Mag.* **2017**, *34*, 72–84. [CrossRef]

16.   Vincent, F.; Vilà-Valls, J.; Besson, O.; Medina, D.; Chaumette, E. Doppler-aided positioning in GNSS receivers—A performance analysis. *Signal Process.* **2020**, *176*, 107713. [CrossRef]

17.   Compagnoni, M.; Notari, R.; Antonacci, F.; Sarti, A. On the statistical model of source localization based on Range Difference measurements. *J. Frankl. Inst.* **2017**, *354*, 7183–7214. [CrossRef]

18.   Bancroft, S. An Algebraic Solution of the GPS Equations. *IEEE Trans. Aerosp. Electron. Syst.* **1985**, *AES-21*, 56–59. [CrossRef]

19.   Abel, J.; Chaffee, J. Existence and uniqueness of GPS solutions. *IEEE Trans. Aerosp. Electron. Syst.* **1991**, *27*, 952–956. [CrossRef]

20.   Chaffee, J.; Abel, J. On the exact solutions of pseudorange equations. *IEEE Trans. Aerosp. Electron. Syst.* **1994**, *30*, 1021–1030. [CrossRef]

21.   Ruggiero, M.L.; Tartaglia, A.; Casalino, L. Geometric definition of emission coordinates. *Adv. Space Res.* **2022**, *69*, 4221–4227. [CrossRef]

22.   Feng, J.C.; Hejda, F.; Carloni, S. Relativistic location algorithm in curved spacetime. *Phys. Rev. D* **2022**, *106*, 044034. [CrossRef]

23.   Serrano Montesinos, R.; Morales-Lladosa, J.A. *Bancroft's GPS Navigation Solution: Relativistic Interpretation*; I.U. de Matemática Multidisciplinar, Universitat Politècnica de València: València, Spain, 2023; pp. 150–157.

24.   Coll, B.; Pozo, J.M. General Causal Properties of Emission Coordinates. Private Communication, 2006.

25.   Coll, B.; Ferrando, J.J.; Morales-Lladosa, J.A. Newtonian and relativistic emission coordinates. *Phys. Rev. D* **2009**, *80*, 064038. [CrossRef]